Adsorption and ODH reaction of alkane on sol–gel synthesized TiO₂–WO₃ supported vanadium oxide catalysts: *In situ* DRIFT and structure–reactivity study

Debaprasad Shee, Goutam Deo*

Department of Chemical Engineering, Indian Institute of Technology Kanpur, Kanpur, 208 016, U.P., India

ABSTRACT

A titania-based mixed-oxide support containing 90 wt% TiO₂, 90Ti–W, and several supported vanadium oxide (vanadia) catalysts, xV90Ti–W (x = 1–12.5 wt% vanadia), were synthesized and characterized. The anatase phase in the 90Ti–W support remained unaffected up to 1073 K. The presence of vanadia, however, leads to an appearance of the rutile phase and a decrease in the catalyst surface area. The xV90Ti–W catalysts possess surface vanadium and tungsten oxide dispersed species at moderate calcination temperatures. At high vanadia loadings, some interaction between the surface vanadium and tungsten oxide species may exist though bulk supported oxides were not detected. During ethane and propane adsorption, at relatively low adsorption temperatures, acetaldehyde and acetone species were observed, which then oxidized to other adsorbed oxygenated species at higher temperatures. Propane oxidative dehydrogenation (ODH) reaction studies revealed that the propene yield measured at the same conversion increased with increasing loading up to 10 wt% vanadia and then decreased. Analysis of the kinetic parameters showed that the rate constant ratio of propene formation to propene combustion, k_1/k_2, which represents the propene yield at the same conversion, also increased with vanadia loading. The 10V90Ti–W catalyst was the best amongst this series of catalysts for the propane ODH reaction in terms of activity and propene yield.

© 2009 Published by Elsevier B.V.

1. Introduction

Supported vanadia catalysts are commonly used in various industrial applications, particularly selective catalytic oxidation and selective catalytic reduction processes [1–6]. The pure titania type in anatase form is usually suitable as a support for several of these applications. The anatase support, however, has limited surface area and undergoes a transformation to the rutile phase at high temperature. Therefore, mixed-oxide support containing titania as a major component has received considerable attention [7–9]. It has been suggested that the presence of tungsten in the mixed-oxide improves the catalytic activity and the thermal stability of titania [9]. Furthermore, the presence of tungsten may provide a promotional effect for some reactions [10].

The tungsten oxide may be present in the mixed-oxide support as dispersed surface tungsten oxide species or crystalline WO₃ particles [11]. The addition of vanadia to a titania-tungsten mixed-oxide support may or may not result in the formation of an isolated species and/or polymeric species as commonly observed on oxide

supports. Furthermore, the surface vanadia species may also interact with the tungsten oxide phase forming a vanadia tungsten oxide compound of general formula W$_x$V$_y$O$_z$ [9,12]. The presence of such compounds may also affect the catalytic performance. Thus, to understand this system in greater detail it is useful to investigate the effect of using a titania-tungsten mixed-oxide support for synthesizing supported vanadia catalysts.

In the present study, a titania-tungsten oxide support was synthesized by the sol–gel method and characterized. A series of mixed-oxide supported vanadia catalysts of various loadings were synthesized by the incipient wetness impregnation method and were also characterized. These mixed-oxide supported vanadia catalysts were probed by the propane ODH reaction. To gain additional insights into the structure–reactivity relationship, certain diffuse reflectance infrared Fourier transform (DRIFT) experiments of ethane and propane adsorption were also undertaken. Infrared studies are particularly useful to elucidate the surface adsorbed species involved [13,14]. Specifically, *in situ* IR spectroscopy has been used for alkane and alkene oxidation processes on various supported metal oxide catalysts to detect the surface oxygenate species [15–19]. Based on these studies, the structure–reactivity relationship for the vanadia catalyst supported by titania-tungsten mixed-oxide is proposed.

* Corresponding author. Tel.: +91 512 2597881; fax: +91 512 2590104.
E-mail address: goutam@iitk.ac.in (G. Deo).

2. Experimental

2.1. Material synthesis

The 90 wt% titania-tungsten support (90Ti–W) was synthesized by the sol–gel method. The precursors used for titania and tungsten oxide were titanium ethoxide (Sigma–Aldrich, 97% purity) and ammonium meta tungstate, respectively. Cetyltrimethylammonium bromide (CTAB, Sigma–Aldrich) was used as a surfactant/template.

In this sol–gel synthesis route, measured quantities of titanium ethoxide and ammonium meta tungstate precursors were added to a mixture of CTAB and absolute ethanol (99.99%). The resulting mixture was stirred for 45 min. A HNO_3/H_2O mixture was used as a hydrolyzing agent and was added drop-wise to the precursor mixture with continuous stirring. The gel formed was aged for 24 h. The molar ratio of titanium ethoxide, CTAB, HNO_3, H_2O, and ethanol in the mixture was 1:0.2:1.5:10:20. After completion of aging, a mixture of NH_4OH and double-distilled water was added to the gel. The mixture was refluxed at 353 K for 48 h. The pH of the mixture was maintained between 9 and 10 during the reflux period. The white precipitate obtained from the mixture was filtered and dried overnight in a vacuum desiccator. A white cake was formed, which was further dried at 333 K for 8 h and at 383 K for 6 h. The dried cake was ground in a mortar and pestle to make a powder. The powdered mixed-oxide support was finally calcined at 723 K.

The 90Ti–W supported vanadia catalysts of various loadings (2–12.5 wt%) were synthesized by the incipient wetness impregnation method. The precursor used for vanadium oxide was a vanadium oxalate solution, which was prepared by mixing a stoichiometric amount of ammonium meta-vanadate (NH_4VO_3, 98% purity) and oxalic acid. The pretreated mixed-oxide support was intimately mixed with an incipient wetness volume of the vanadium oxalate solution. The paste formed was dried at room temperature overnight and at 383 K for 6 h. Additional details of the catalyst synthesis are given elsewhere [20]. The catalysts were finally calcined at 723 K. The catalysts were denoted as xV90Ti–W, where x represents the wt% of vanadia as V_2O_5 present in the catalysts. To observe the effect of calcination temperatures, the synthesized xV90Ti–W (x = 0–10 wt%) catalysts were also calcined for 3 h at different temperatures that ranged from 723 to 1073 K.

2.2. Surface area measurement

The BET surface area of all the samples was determined by nitrogen adsorption using the single point BET equation. The adsorption gas was a 30% N_2/He gas mixture. A QUANTACHROME (Model no: OS-7) BET surface area analyzer equipped with a QUANTACHROME mass flow controller module (Model no: LMFC-7) was used for these studies. Sample amounts ranging from 100 to 250 mg were degassed at 423 K in flowing nitrogen before nitrogen adsorption at 77 K was carried out.

2.3. X-ray diffraction (XRD)

The XRD patterns of all the samples were obtained in the range of 10–70° with a scanning speed of 3° min^{-1} on an ISO Debye Flex-2002 X-ray diffractometer using Cu Kα irradiation (λ = 1.54056 Å).

2.4. Raman spectroscopy

The Raman spectra of the samples were obtained using a Raman spectrometer (Horiba-Jobin Yvon LabRam–HR) equipped with a confocal microscope, 2400/900 grooves/mm grating, and a notch filter. A 532-nm (visible) Yag double-diode pumped laser source was used for excitation. All spectra were obtained at a resolution

of ~2 cm^{-1}. The powdered samples were placed in a high temperature *in situ* cell (Linkam THMS-1600) to obtain the spectra under dehydrated conditions. The samples were heated to 673 K in a flow of 10% O_2/Ar for 30 min before the Raman spectra were collected.

2.5. Fourier transform infrared spectroscopy (FTIR)

2.5.1. Dehydrated spectra

The IR spectra of the samples under dehydrated conditions were obtained using a BRUKER TENSOR 27 FTIR spectrometer coupled with a diffuse reflectance accessory (HARRICK Praying Mantis, DRP-BR4) and a high temperature reaction chamber (HARRICK HVC-DRP-2) equipped with KBr windows. For obtaining the dehydrated IR spectra, the sample cup of the reaction chamber was filled with the powdered sample. Oxygen gas was then introduced into the reaction chamber at a flow rate of 30 ml/min. The temperature of the reaction chamber was gradually raised to and maintained at 673 K for 1 h by an automatic temperature controller module (HARRICK ATC-024-2). All the spectra were recorded against a KBr background at a resolution of 4 cm^{-1} using 128 scans.

2.5.2. FTIR adsorption studies

The *in situ* FTIR adsorption studies with the xV90Ti–W samples were performed using ethane or propane as the adsorbate in the same experimental setup described above. The samples were pretreated in the reaction chamber at 673 K for 45 min in oxygen flowing at 30 ml/min. After pretreatment, the sample was cooled to room temperature. The gas line and reaction chamber were then purged by flowing of helium (or nitrogen) gas. A gas mixture containing alkane (ethane or propane) and helium (or nitrogen) was then introduced into the reaction chamber. The temperature of the reaction chamber was varied from 293 to 633 K using an alkane (ethane or propane) partial pressure of 0.2 atm and helium as the diluent. Adsorption studies were also performed from 573 to 633 K, using different adsorbates (ethane or propane) with the partial pressure varying from 0.05 to 0.6 atm. In this instance, nitrogen gas was used as the diluent. The total flow rate of the adsorbate gas mixture was maintained at 30 ml/min and separate mass flow controllers (ALBORG-GFC171S) controlled individual flow rates of each gas stream. The IR spectra were recorded at all adsorption conditions mentioned against: (a) KBr + He (or N_2) and (b) KBr + He (or N_2) + adsorbate (ethane or propane) background. The second background was chosen to eliminate the contribution of gas-phase adsorbate from the overall spectra. The resolution and number of scans were the same as noted above.

2.6. Temperature programmed reduction (TPR)

Temperature programmed reduction studies of the xV90Ti–W catalysts using hydrogen as the reducing agent were carried out in a Micromeritics Pulse Chemisorb 2705 apparatus. Samples of 25–35 mg were loaded in a U-tube quartz reactor. Before reduction, all the samples were pretreated in flowing Ar (30 ml/min) at 473 K for 30 min to remove adsorbed moisture and other impurities that may be present. The reactor was then cooled to room temperature. At room temperature, a mixture of 5% H_2–Ar gas mixture at 30 ml/min was introduced into the quartz reactor. The sample was heated up to 1200 K using a temperature programmed rate of 10 K/min. The hydrogen consumption was quantitatively monitored by using a thermal conductivity detector.

2.7. Reaction studies

The ODH reaction was carried out in a fixed bed, down-flow, isothermal tubular quartz reactor at atmospheric pressure. Three separate mass flow controllers (Bronkhorst Hi-Tech, E1 mass flow

controllers) were used to control the flow rates of the inlet gas (propane, nitrogen, and oxygen). Two types of reaction studies were conducted: contact time and kinetic parameter estimation. An inlet-gas flow rate range of 30–120 ml/min was used for contact time studies and a total flow rate of 75 ml/min for kinetic parameter estimation studies. Contact time studies were carried out at 653 K using a propane-to-oxygen molar ratio of 2:1. For kinetic studies, the reaction temperature was varied from 613 to 673 K and the propane-to-oxygen molar ratio was varied from 1:1 to 3:1. Nitrogen was used as a diluent and its quantity was adjusted with oxygen such that the inlet-gas composition corresponded to that of air. The propane conversions were maintained below 10% to ensure minimal mass and heat transfer effects. Blank experiments were also carried out at identical reaction conditions to ensure no homogeneous contribution of the reaction occurred. Additional details of the reactor setup, calculations for conversion, selectivity, yield, and kinetic parameters estimation can be found elsewhere [20–22].

3. Results and discussion

3.1. Characterization of mixed-oxide support and supported vanadia catalysts

The surface area and the corresponding surface vanadia densities (V atoms/nm^2) of the xV90Ti–W samples are presented in Table 1. Data from TPR studies, T_{max}, and reaction studies, ψ, are also included in Table 1. It is observed from Table 1 that the surface area of the mixed-oxide supported vanadia catalysts decreases as the vanadia loading is increased. The calculated vanadia surface densities based on the specific surface area of the 90Ti–W support range from 1.0 to 6.3 V atoms/nm^2.

The surface areas of the samples calcined from 723 to 1073 K were also determined. With an increase in calcination temperature, the surface areas of the samples decreased. However, the specific decrease in surface area occurs differently for each sample. To compare the relative decrease, the surface areas were normalized to the surface area of the corresponding sample measured at 723 K. The normalized surface areas of the samples for different calcination temperatures are shown in Fig. 1. From Fig. 1 it is observed that for the 90Ti–W support the surface area is relatively constant up to a calcination temperature of 873 K and gradually decreases thereafter. The surface areas of the xV90Ti–W catalysts, however, continuously decrease with an increase in calcination temperature. Furthermore, the decrease of surface areas depends on the vanadia loading; the higher the vanadia loading the more rapid is the decrease in surface area with an increase in calcination temperature. It appears that the higher mobility of the surface vanadia phase accelerates the surface area decreases.

The 90Ti–W support and xV90Ti–W catalysts, calcined at different temperatures, were also characterized by XRD. The XRD patterns for the 90Ti–W support, calcined at different temperatures, are shown in Fig. 2 and reveal that only the anatase phase is present even up to 1073 K. These results suggest that the anatase phase of titania is stable even up to 1073 K though the support
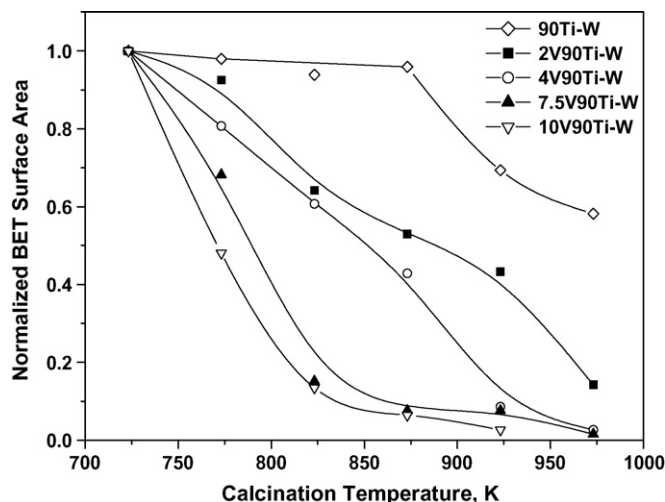

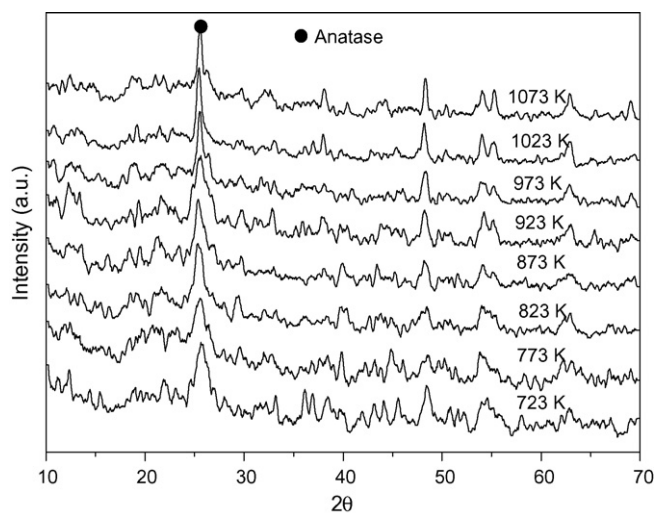**Fig. 1.** Normalized BET surface area versus calcination temperature for xV90Ti–W catalysts.

Fig. 2. XRD patterns of 90Ti–W support calcined at different temperatures.

surface area decreases. The xV90Ti–W catalysts, however, show the presence of the rutile phase. The 2V90Ti–W catalyst possesses the titania anatase phase up to 1023 K, small amounts of rutile at 1023 K, and only the rutile phase at 1073 K. For the 4V90Ti–W, 7.5V90Ti–W, and 10V90Ti–W catalysts, the rutile phase appears at 923 K and only the rutile phase is present at 973 K. These results suggest that the surface vanadia species facilitate the anatase to rutile phase transformation. Furthermore, on correlating the surface areas and changes in XRD patterns it appears that the anatase to rutile transformation and the decrease in surface area are not directly correlated.

Table 1
Particulars of the 90Ti–W support and xV90Ti–W catalysts.

Nomenclature	V$_2$O$_5$ (wt%)	Surface area (m^2/g)	Surface density^a (V atoms/nm^2)	T_{max} (K)	CO$_2$/CO, ψ
90Ti–W	0.0	151	0	795, 1067	–
2V90Ti–W	2.0	134	1.0	732, 806, 1069	0.96
4V90Ti–W	4.0	140	1.8	731, 820, 1065	0.77
7.5V90Ti–W	7.5	132	3.5	732, 820, 988, 1068	0.56
10V50Ti–W	10.0	104	5.8	744, 820, 988	0.47
12.5V50Ti–W	12.5	60	6.3	757, 820, 987	–

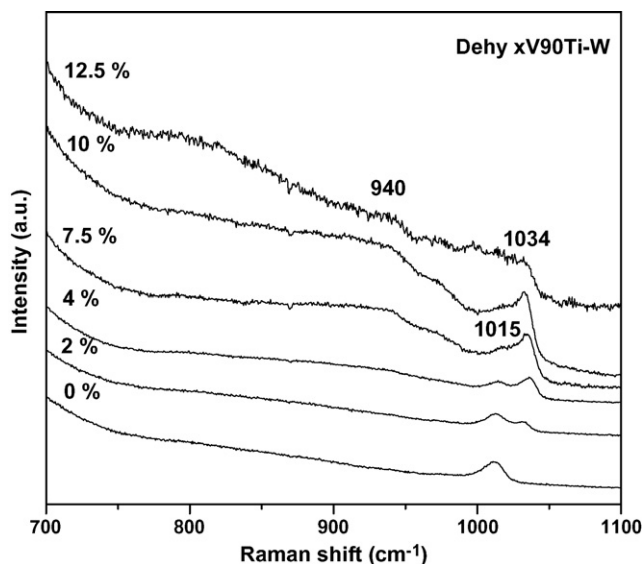^{a} Surface density is calculated based on mixed-oxide support surface area.

Fig. 3. Raman spectra of dehydrated xV90Ti–W ($x = 0$–12.5 wt%) catalysts.

The Raman spectra of the 90Ti–W support and xV90Ti–W catalysts were obtained under dehydrated conditions. The spectra for all dehydrated samples are shown in the 700–1100 cm^{-1} region in Fig. 3. The spectrum of the dehydrated 90Ti–W support reveals a Raman band at 1015 cm^{-1} which is characteristics of W=O vibrations arising from polytungstates [23]. For the xV90Ti–W catalysts, a Raman band is observed at 1034 cm^{-1} due to the terminal V=O bond vibration of the surface vanadia species [24]. A band at ~940 cm^{-1} is also observed, which was assigned to V–O–support vibrations [25]. At high vanadia loadings the W=O and V=O Raman bands are not discernible, which may be related to the loss of surface vanadium and tungsten oxide species. Furthermore, Raman bands due to bulk V$_2$O$_5$ and WO$_3$ are absent suggesting that the vanadium and tungsten oxide species are present as dispersed phases. It is also possible that some of the tungsten oxide is present as a dispersed phase in the titania matrix and is not readily detected by Raman spectroscopy [26,27].

The FTIR spectra of dehydrated 90Ti–W support and xV90Ti–W catalysts are reproduced in Fig. 4. Under dehydrated conditions, vibrations less than 1500 cm^{-1} are not discernible in the present DRIFT setup. The IR spectrum of the dehydrated 90Ti–W sup-
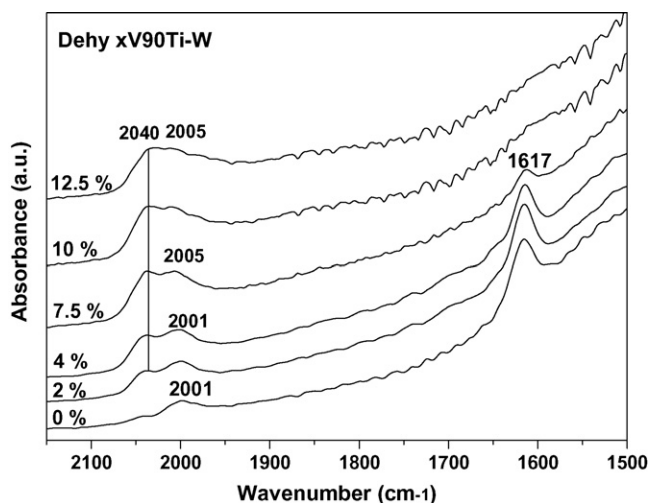
port in Fig. 4 reveals an unassigned vibration band at ~1617 cm^{-1}, whose intensity diminishes with increase in vanadia loading. This ~1617 cm^{-1} band is not due to adsorbed moisture since it persists even at 673 K. This band is also observed in some of the adsorption studies discussed later. Also observed is a 2001 cm^{-1} band arising from the surface tungsten oxide species and assigned to the first overtone band of W=O bond vibration [12,24]. For the xV90Ti–W catalysts, two distinct bands at 2040 and 2001–2005 cm^{-1} are observed. These IR bands at 2040 and 2001–2005 cm^{-1} are assigned to the first overtone V=O and W=O terminal bond vibrations, respectively [24]. A slight shift of the W=O overtone band to higher wavenumber occurs for the supported vanadia catalysts and has been observed by others [24]. It appears that the V=O band intensity increases with an increase in vanadia loading and overshadows the W=O band at higher vanadia loading. A detailed analysis of the overtone IR bands reveals that the V=O band intensity increases till 7.5 wt% loading, is relatively constant for the 10 wt% loading sample, and then decreases for the 12.5V90Ti–W catalyst. The 7.5 wt% loading sample corresponds to 3.5 V atoms/nm^2. The relatively constant intensity for the 10V90Ti–W catalyst and decrease in intensity for the 12.5V90Ti–W catalyst may be associated with the formation of a dispersed vanadia species that is not readily detected by the Raman and IR spectroscopy techniques.

The H$_2$-TPR profiles of all the samples are shown in Fig. 5 and the corresponding temperature maxima values, T_{max}, are tabulated in Table 1. For the 90Ti–W support at 795 and 1067 K, two T_{max} values were observed. These two reduction peaks are attributed to the stage-wise reduction of the surface tungsten oxide species on titania [27]. Addition of vanadia on the 90Ti–W support gradually shifts the T_{max} peak from 795 to ~820 K. With an increase in vanadia loading the intensity of the T_{max} peak at ~1067 K due to the 90Ti–W support decreases and a T_{max} peak at 731–757 K increases. The T_{max} peak at 731–757 K is due to the surface vanadia species. For samples possessing vanadia loading of 7.5 wt% level and higher another T_{max} peak at ~988 K was also observed. The origin of this T_{max} peak at ~988 K is unknown. This peak cannot be assigned to bulk V$_2$O$_5$ since bulk V$_2$O$_5$ possesses T_{max} peaks at ~840, 950, and 1075–110 K [28]. However, considering the ranges in T_{max} temperatures of various supported metal oxides it appears that this T_{max} peak originates from the reduction of the tungsten oxide species. Furthermore, it appears that the T_{max} peak at ~988 K increases at the expense of the T_{max} peak at ~1067 K and may be associated with the T_{max} peak at ~920 K observed previously for a WO$_3$/TiO$_2$ system [29]. It is possible that the
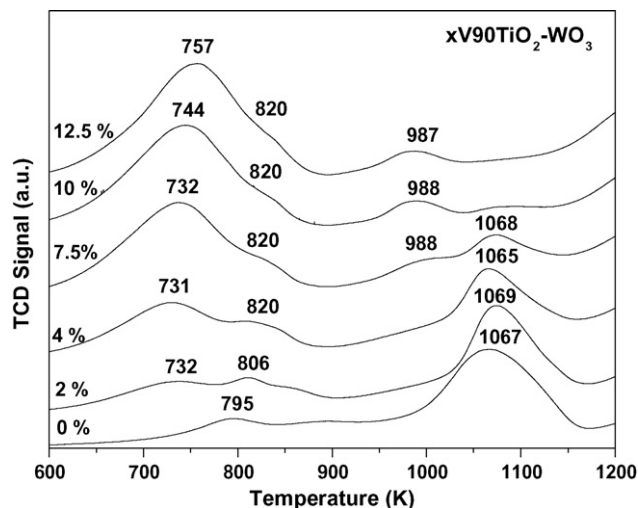

Fig. 4. FTIR spectra of dehydrated xV90Ti–W catalysts ($x = 0$–12.5 wt%). Spectra were obtained at 673 K.

Fig. 5. TPR profile of the xV90Ti–W catalysts ($x = 0$–12.5 wt%).

T_{max} peak at ~988 K is due to a tungsten oxide species interacting with the vanadium oxide species. The presence of this peak may have the same origin as the undetected dispersed vanadia species in the 10V90Ti–W and 12.5V90Ti–W sample as mentioned above.

3.2. In situ FTIR adsorption studies of hydrocarbons

In situ IR studies were carried out to monitor the various species formed during ethane and propane adsorption on various samples. The DRIFT spectra revealed IR bands in two distinct regions: 3100–2700 and 2000–1100 cm^{-1}. The IR bands obtained in the 3100–2700 cm^{-1} region are primarily due to gas-phase adsorbates (ethane or propane). The bands in this region disappear when KBr + He (or N$_2$) + adsorbate are used as the background spectra. Furthermore, the intensity of the IR bands in this region rises with an increase in adsorbate partial pressure, confirming that these bands are due to the gas-phase molecules. For brevity, the IR spectra in this region are not shown. Several studies exist in the literature addressing the nature of alkane-based adsorbed species. Based on these studies the IR bands of various adsorbed species relevant to the present study are tabulated in Table 2. This tabulation assists in the assignment of the various bands observed in the DRIFT spectra of Figs. 6–9. In Figs. 6–9, it should be noted that an unassigned band at ~1615 cm^{-1} was observed (see also Fig. 4). Furthermore, an IR band at 1629–1620 cm^{-1}, associated with adsorbed moisture is also observed and the intensity of this moisture band diminishes with an increase in temperature.

3.2.1. Ethane adsorption studies

Adsorption of ethane on the 90Ti–W support shown in Fig. 6 reveals several IR bands in the 1100–2000 cm^{-1} region. The spectra were recorded over a temperature range of 293–633 K using an ethane partial pressure of 0.2 atm. Based on the compilation given in Table 2, the bands at 1680, 1411 (weak), 1370, and 1240 cm^{-1} are assigned to the adsorbed acetaldehyde species [30]. The intensity of the 1680 cm^{-1} band initially rises and then diminishes with an increase in temperature. At 573 K, the adsorbed acetaldehyde bands disappear suggesting that acetaldehyde undergoes further conversion. The IR bands at 1522, 1440, and 1350 cm^{-1} are assigned to the adsorbed acetate species [16,31]. Of these three, the band at 1350 cm^{-1} is weak and not clearly discernable at lower adsorption temperatures. At 603 K, two new bands at 1850 and 1780 cm^{-1} are observed that are typical of adsorbed cyclic anhydrides species [32].
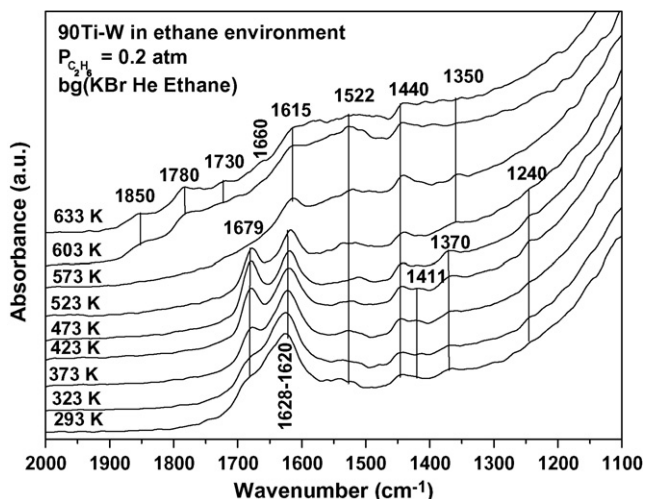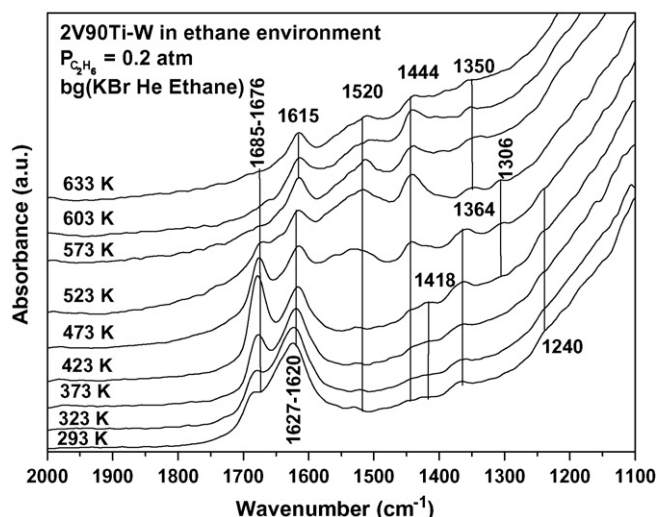

Fig. 7. DRIFT spectra of adsorption of ethane on 2V90Ti–W catalyst. T = 293–633 K; $P_{C_2H_6}$ = 0.2 atm.

Two additional weak bands are observed at 1660 and 1730 cm^{-1} for 90Ti–W at 603 K and above. The 1660 cm^{-1} band may be due to a C=O vibration conjugated with a double bond or νC=C vibration of olefins. The weak 1730 cm^{-1} band is assigned to a νC=O bond vibration of aldehydes or ketones and is reported as the intermediate species towards adsorbed cyclic anhydride formation [32]. Similar bands are obtained for ethane adsorption studies performed at different ethane partial pressures.

Adsorption of ethane on supported vanadia catalysts, xV90Ti–W, were also studied under similar conditions. The DRIFT spectra of ethane adsorption on 2V90Ti–W using an ethane partial pressure of 0.2 atm and temperatures ranging from 293 to 633 K is shown in Fig. 7 and reveal several bands in the 1200–1700 cm^{-1} region. Using Table 2, the IR bands at 1685–1676, 1418 (weak), 1364, and 1240 cm^{-1} are assigned to the adsorbed acetaldehyde species [30]. For 4V90Ti–W, 7.5V90Ti–W, and 10V90Ti–W the 1685–1676 cm^{-1} band gradually shifts to 1660–1650 cm^{-1} at 523 K and above (spectra not shown). Moreover, the bands at 1364 and 1240 cm^{-1} disappear at 523 K and above. The bands at 1520, 1444,
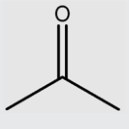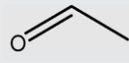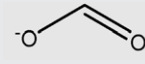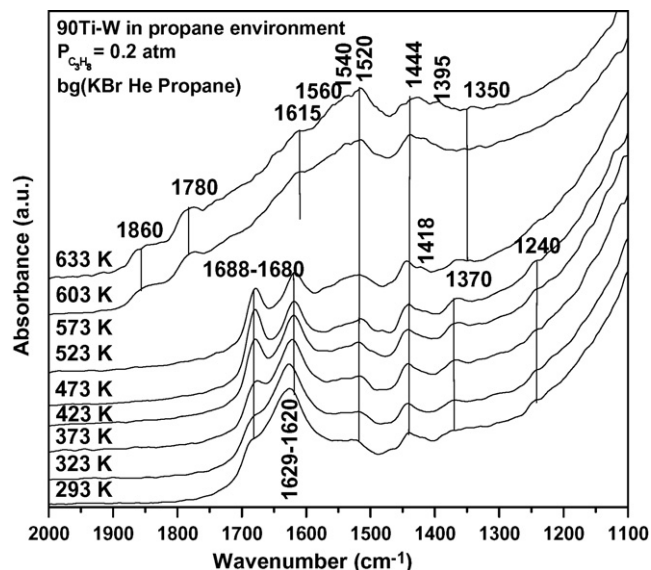

Fig. 6. DRIFT spectra of adsorption of ethane on 90Ti–W support. T = 293–633 K; $P_{C_2H_6}$ = 0.2 atm.

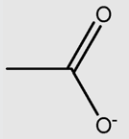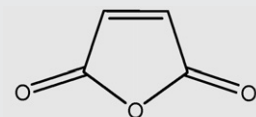**Fig. 8.** DRIFT spectra of adsorption of propane on 90Ti–W support. T = 293–633 K; $P_{C_3H_8}$ = 0.2 atm.

Table 2
IR bands of surface species relevant to the present study.

Surface species	Structure	Mode of vibration	IR band (cm^{-1})	Ref.
Acetone		$\nu C=O$	1690–1680	[13]
		$\nu_a C-C$	1240	
		$\delta_a CH_3$	1420	
		$\delta_s CH_3$	1366	
Acetaldehyde		$\nu C=O$	1690–1680	[29]
		$\nu_a C-C$	1240	
		$\delta_a CH_3$	~1330	
		$\delta_s CH_3$	~1370	
Formate		$\nu_a COO^-$	1560, 1590	[31]
		$\nu_s COO^-$	1350	
		$\delta C-H$	~1400	
Acetate		$\nu_a COO^-$	1515, 1540–1530	[16,31]
		$\nu_s COO^-$	1440–1445	
		δCH_3	1350	
Cyclic anhydride		$\nu_a OCOCO$	~1860	[30]
		$\nu_s OCOCO$	~1785	
Olefin	$(-C=C-)$	$\nu C=C$	1660–1640	[31]

and 1350 cm^{-1}, assigned to adsorbed acetate, are distinct at 523 K. The intensities of the acetate bands initially rise and then diminish as the temperature increases. The IR bands corresponding to adsorbed acetate species are well defined on the xV90Ti–W catalysts compared to those corresponding to the 90Ti–W support. Furthermore, the IR bands due to cyclic anhydrides are not observed on the xV90Ti–W catalysts.

Adsorption of ethane on the 90Ti–W support and xV90Ti–W catalysts revealed the presence of various adsorbed oxygenated species in the 293–633 K temperature range and 0.2 atm ethane partial pressure. The main adsorbed oxygenate species formed were

Fig. 9. DRIFT spectra of adsorption of propane on 2V90Ti–W catalyst. $T = 293$–633 K; $P_{C_3H_8} = 0.2$ atm.

acetaldehyde, acetate, and cyclic anhydride. It has been suggested that the adsorption of ethane on oxide surfaces occurs by the abstraction of the hydrogen atom to form an adsorbed ethoxide species, which is the precursor of ethylene [18]. Further oxidation of the ethoxide species produces the acetaldehyde species. The adsorbed acetaldehyde species further oxidizes to the acetate species. The adsorbed acetate species can coordinate to the catalyst surface as a monodentate or bidentate species, which can be inferred from the splitting of the acetate stretching vibration [33]. Based on the splitting of the acetate stretching vibration, 75–100 cm^{-1}, it appears that bidentate linkages exist though monodentate linkages cannot be disregarded. Cyclic anhydride species are formed only on the 90Ti–W support at 603 K and above. The cyclic anhydride species are the precursors for CO_2 formation [19]. The complete absence of or the presence of only a low IR band intensity of cyclic anhydride species for the xV90Ti–W catalysts suggests that one of the routes for CO_2 formation from the support during ethane oxidation is suppressed by the surface vanadia species. Consequently, a decrease in the CO_2 formation from the support is to be expected.
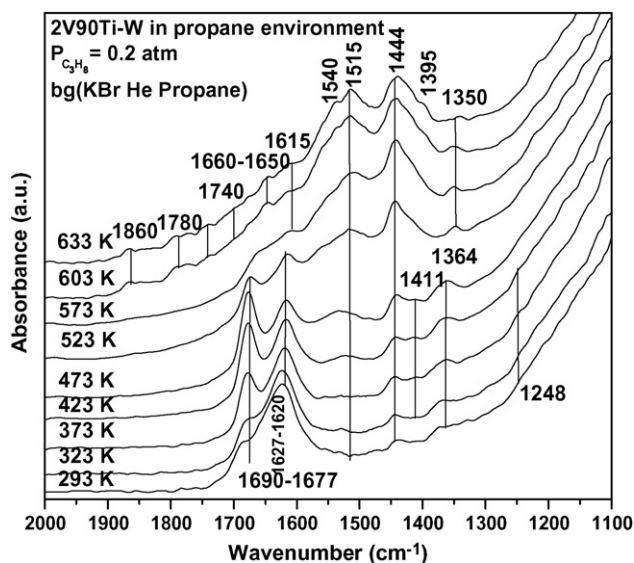
3.2.2. Propane adsorption studies

Similar to ethane adsorption, the adsorption of propane on the 90Ti–W support and xV90Ti–W catalysts shown in Figs. 8 and 9 reveals several IR bands in the 1100–2000 cm^{-1} region. The IR bands at 1688–1680, 1418, 1370, and 1240 cm^{-1} are bands typical of adsorbed acetone species (see Table 2). These bands disappear at 573 K and above. The IR bands at 1520, 1444, and 1350 cm^{-1} suggest the formation of acetate species and the intensities of the first two bands rise as the adsorption temperature increases. The IR band at 1350 cm^{-1} is not observed below 523 K. An IR band at 1540 cm^{-1} is also observed at 573 K and higher temperatures due to the acetate species. At 633 K a weak band at 1560 cm^{-1} appears, which together with the bands at 1350 and 1395 cm^{-1} are assigned

to the formate species. Two new bands at ~1860 and ~1780 cm^{-1} appear at an adsorption temperature of 603 K and are typical of cyclic anhydride species. As in ethane adsorption, two bands at 1650 and 1740–1730 cm^{-1} (see Fig. 9) are observed at 633 K. Accordingly, the 1650 cm^{-1} band arises from a νC=C vibration of olefin or νC=O vibration of a carbonyl group conjugated with a double bond [32]. The presence of the 1650 cm^{-1} band suggests that adsorbed aldehyde/ketone-like species may be present. The IR band at 1730–1740 cm^{-1} band is assigned to the νC=O vibration of an intermediate species towards the formation of cyclic anhydride. The presence of acrylate species, which is expected at 1640 (νC=C), 1500 (ν_{as}COO$^-$), 1440 (ν_sCOO$^-$), 1370, and 1270 (δCH) cm^{-1}, is unsubstantiated since other IR bands typical of the acrylate species are absent [31].

Comparing the 90Ti–W with the xV90Ti–W spectra reveals similarities and differences. Though the same oxygenated species (acetone, acetate, formate, and cyclic anhydride) are observed, their intensities are different. For the xV90Ti–W catalysts, the IR band intensities of the acetone, acetate, and formate species are higher and the IR band intensity of the adsorbed cyclic anhydride species is lower compared to that of the 90Ti–W support. Resini et al. reported that the adsorbed isopropoxide species is formed on adsorption of isopropyl alcohol [13]. At 473 K and above the isopropoxide species is converted to acetone. The formation of acetone species in the present study suggests that it is formed due to the further oxidation of isopropoxide species. Furthermore, the present results suggest that the formation of isopropoxide is the first step of propane adsorption. Adsorption of propane on 90Ti–W support and xV90Ti–W catalysts was also studied at partial pressures of propane ranging from 0.05 to 0.6 atm and temperatures from 573 to 633 K. These results reveal that the band intensities typical for acetate, formate, and cyclic anhydride species rise with increase in partial pressure of propane suggesting that growth of the oxygenated species is a function of propane partial pressure.

3.3. Propane ODH reaction studies

The propane ODH reaction was conducted at different contact times over the xV90Ti–W catalysts and the results are shown in Fig. 10. The propane conversion increases with increase in contact time and at the same contact time, the propane conversion increases with increase in vanadia loading until it reaches the 7.5 wt% level, is constant for the 10 wt% loading and decreases thereafter. The trend in propane conversion measured at the same contact time is as follows:

$$2V90Ti\text{-}W < 4V90Ti - W < 12.5V90Ti - W \leq 7.5V90Ti$$
$$- W \approx 10V90Ti - W.$$

A similar trend of propene yield with contact time is also observed and is not shown here for the sake of brevity. The variation in propane conversion and propene yield with loading is consistent with the amounts of the surface vanadia species observed by characterization studies. The relatively similar conversion values for 7.5V90Ti–W and 10V90Ti–W and the decrease in conversion for the 12.5V90Ti–W are consistent with the dehydrated IR band intensities of the surface vanadia species observed in Fig. 4. Contact time studies also reveal that the yield of CO$_2$ measured at the same conversion decreases with increase in vanadia loading. This observation correlates well with the findings in the DRIFT studies using propane since the cyclic anhydride species, one of the possible precursors for the CO$_2$ formation, decreases with increase in vanadia loading. Consequently, one of the routes for the formation of CO$_2$ is suppressed when the vanadia loading is increased.

The effect of catalyst calcination temperature on the propane ODH reaction over xV90Ti–W was also studied. Four catalysts, 2V90Ti–W, 4V90Ti–W, 7.5V90Ti–W, and 10V90Ti–W calcined at temperatures ranging from 723 to 1073 K were considered for this purpose. To study the effect of calcination temperatures, the propane ODH reaction was carried out at 673 K using a propane-to-oxygen molar ratio of 2:1 and a total gas flow rate of 75 ml/min. It was observed that at high calcination temperatures the catalysts deactivate. However, the specific deactivation differs for each catalyst. To observe the relative deactivation for the different catalysts the propene yield is normalized with respect to the propene yield obtained for the same catalyst calcined at 723 K. The normalized propene yield as a function of calcination temperature for the four catalysts is shown in Fig. 11. The propene yield for 2V90Ti–W is relatively constant until a calcination temperature of 823 K, and at higher calcination temperatures the propene yield gradually decreases. For 4V90Ti–W, 7.5V90Ti–W, and 10V90Ti–W the propene yield starts to decrease at progressively lower temperatures. Besides, the decrease of propene yield with calcination
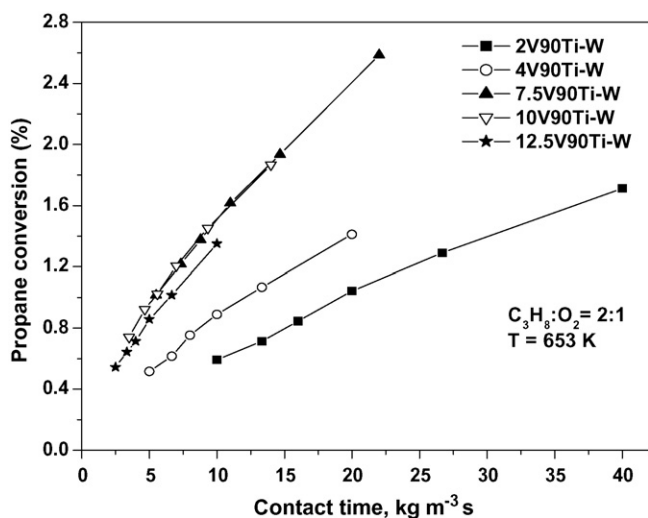

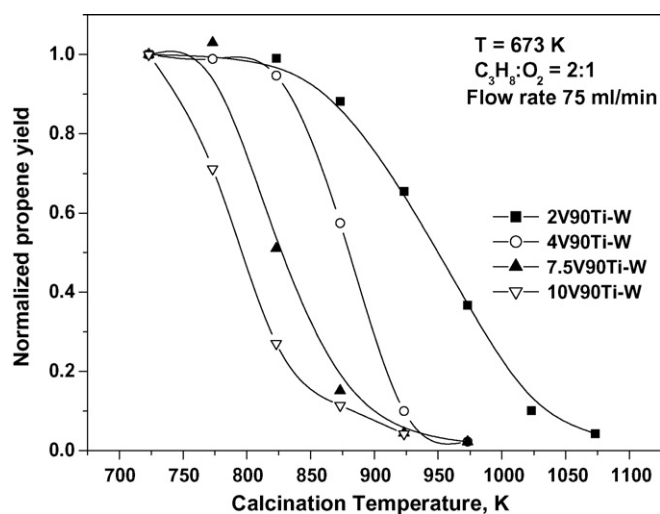**Fig. 10.** Variation of propane conversion with contact time for xV90Ti–W (x = 2–12.5 wt%) catalysts.

Fig. 11. Normalized propene yield versus calcination temperature for xV90Ti–W catalysts.

Table 3
Kinetic parameter values of the titania-tungsten mixed-oxide supported vanadia catalysts. Standard errors are given in parenthesis. $T_m = 643.15$ K.

| Parameter	Units	Catalysts			
		2V90Ti–W	4V90Ti–W	7.5V90Ti–W	10V90Ti–W
k_{10}		27 (3)	72 (4)	98 (6)	117 (5)
k_{20}	ml STP min^{-1} (g cat)$^{-1}$ atm^{-1}	1089 (57)	1792 (75)	2411 (100)	2302 (105)
k_{30}		1101 (50)	313 (60)	721 (73)	822 (76)
k_{10}/k_{20}	–	0.025	0.04	0.041	0.051
E_1		84 (7)	67 (6)	72 (6)	59 (3)
E_2	kJ mol^{-1}	30 (8)	45 (8)	61 (11)	51 (10)
E_3		80 (7)	121 (20)	144 (19)	108 (13)
$E_1 - E_2$		54	22	11	8

temperature is related to vanadia loading. These results suggest that the loss of catalytic activity with calcination temperature depends on the vanadia loading, and deactivation increases with increase in loading.

Correlating the information obtained from deactivation with characterization studies reveals that the specific variations of the decrease in surface area, anatase-to-rutile transformation, and catalyst deactivation are different. The deactivation of catalysts, however, is directly related to the loss of surface vanadia species with calcination temperature [28]. The anatase-to-rutile transformation or loss of surface area is not always related to the loss of vanadia sites.

### 3.4. Parameter estimation for propane ODH

The propane ODH kinetic parameters were estimated in order to acquire additional information about the catalysts. A sequential Mars van Krevelan (MVK) reaction model was considered for kinetic parameter estimation. The MVK reaction model considered assumes that the gas-phase propane reacts with the lattice oxygen of the catalysts to produce propene, which is further oxidized by lattice oxygen to produce carbon oxides ($CO + CO_2$). The gas-phase oxygen replenishes the lattice oxygen by re-oxidation of the catalyst. The three reactions, r_1, r_2, and r_3 considered are given below:

1. Formation of propene (r_1):

$$C_3H_8 (g) + O(s) \rightarrow C_3H_6 (g) + H_2O + *_{red} \qquad (1)$$
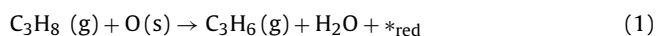
where $*_{red}$ is a reduced site.
2. Formation of carbon oxides, CO_x (r_2):

$$C_3H_6 (g) + 3(x+1)O(s) \rightarrow 3CO_x (g) + 3H_2O + 3(x+1)*_{red} \qquad (2)$$
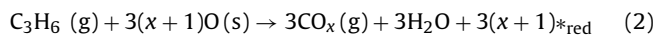
where x is 1 for CO and 2 for CO_2.
3. Catalyst re-oxidation (r_3):

$$O_2 (g) + 2*_{red} \rightarrow 2O(s) \qquad (3)$$

The rate constants associated with the above three reactions are k_1, k_2, and k_3. These k_i's are made up of the respective pre-exponential factors, k_{i0}'s, and activation energies, E_i's.

The CO_2/CO ratios, ψ, used in kinetic parameter estimations are calculated based on the entire reaction data for each catalyst and are shown in Table 1. The value of ψ decreases as vanadia loading increases suggesting that lower amounts of CO_2 are formed at high loadings, which is again consistent with the findings in the DRIFT studies.

The estimated kinetic parameters for the four catalysts are presented in Table 3. The kinetic parameters, k_{i0}'s and E_i's, their units and the associated standard errors are also furnished. Comparisons of standard errors with parameter values in Table 3 suggest that

the kinetic parameter values have been estimated with a reasonable degree of accuracy. Moreover, a comparison between the actual and predicted concentrations of all compounds analyzed reveal that a close correspondence exists for all the catalysts. However, this comparison is not shown for the sake of brevity.

Analysis of the kinetic parameters in Table 3 reveals that they vary with the vanadia loading. The value of the pre-exponential factor for propene formation, k_{10}, increases as the vanadia loading increases. The pre-exponential factor of carbon oxides formation, k_{20}, is also a function of and increases with vanadia loading until it reaches the 7.5 wt% level and then decreases. The activation energy for propene formation, E_1, is the highest for 2V90Ti–W and is relatively constant for 4V90Ti–W and 7.5V90Ti–W. The 10V90Ti–W catalyst has the lowest E_1 value amongst the xV90Ti–W catalysts. The activation energy for carbon oxides formation, E_2, increases with increase in vanadia loading until the latter reaches the 7.5 wt% level and decreases for the 10V90Ti–W catalyst.

Previous studies revealed that the rate constants ratio, k_1/k_2, is an important parameter for understanding the effect of vanadia loading on the propene yield at the same conversion [20,22]. For a series reaction, the propene yield at the same conversion depends on the ratio of rate constants, k_1/k_2 [34]. The rate constants, k_1 and k_2, correspond to the rate constants for reactions (1) and (2) above. The k_1/k_2 ratio for various catalysts in turn depends on the value of k_{10}/k_{20} and difference in activation energies, $E_1 - E_2$, which is temperature-dependent. Due to the reparameterization of E_i's, the k_1/k_2 ratio is equal to the k_{10}/k_{20} ratio at $T = T_m$ [21]. The values of k_{10}/k_{20} and $E_1 - E_2$ are also given in Table 3. At $T = T_m$, the k_{10}/k_{20} ratio is the lowest for the 2V90Ti–W catalyst and is similar for the 4V90Ti–W and 7.5V90Ti–W catalysts. The 10V90Ti–W catalyst has the highest k_{10}/k_{20} value suggesting that at 643 K this catalyst provides the best propene yield at the same conversion. Moreover, from Fig. 10 it is observed that the 10V90Ti–W catalyst also provides the highest conversion measured at the same contact time and appears to be the best amongst this series of catalysts.

At reaction temperatures different from T_m, the variation of the k_1/k_2 ratio depends on the specific $E_1 - E_2$ value. Since all $E_1 - E_2$ values are positive the k_1/k_2 ratio always increases with temperature. However, for each catalyst the specific increase of k_1/k_2 with temperature depends on the specific $E_1 - E_2$ value. A higher $E_1 - E_2$ value suggests that k_1/k_2 is more sensitive to temperature. Thus, for 2V90Ti–W the k_1/k_2 value increases more rapidly than for 10V90Ti–W. Despite this, the k_1/k_2 for the 2V90Ti–W catalyst is always lower than the 10V90Ti–W catalyst in the temperature region considered here. Thus, the 10V90Ti–W is the best amongst this series of catalysts in terms of propane conversion and propene yield in the operating conditions considered, though this catalyst may possess some dispersed undetected vanadia species as observed by the characterization techniques. The amount of the dispersed undetected vanadia species, however, is not known and is expected to be small.
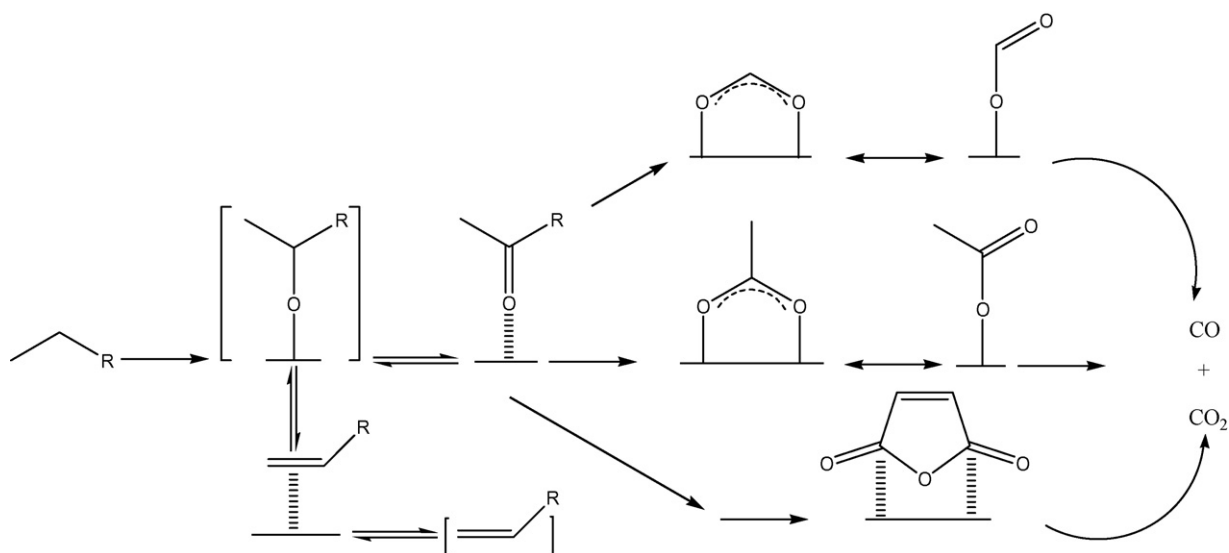
Fig. 12. Possible pathways for the alkane ODH reaction based on DRIFT study of ethane, and propane adsorption. R = H for ethane and R = −CH$_3$ for propane.

4. Conclusions

A series of vanadium oxide catalysts supported on a titania-tungsten mixed-oxide support containing 90 wt% TiO$_2$ were synthesized by the incipient wetness impregnation method and characterized. The BET surface area of the mixed-oxide supported catalysts decreases with increase in vanadia loading. The Raman and FTIR spectra obtained under dehydrated conditions and TPR studies suggest that the tungsten and vanadia species are present as dispersed phases. It appears that the behavior of the 90Ti–W support is similar to the more commonly used supports in the formation of surface vanadia species. The support possesses surface tungsten oxide species and is able to retain its surface area until 873 K is reached; however, the presence of surface vanadia species accelerates the loss of surface area and formation of rutile phase at temperatures lower than those observed for the pure oxide support. A decrease in catalytic activity with rising calcination temperature was also observed; however, such decrease was not directly related to rutile formation or changes in surface area. The decrease in catalytic activity is attributed to the loss of surface vanadia species with increase in calcination temperature, which is not necessarily related to rutile formation or decrease in surface area. Surface vanadia species are formed and the quantities of these species increase with the loading until a level of 7.5 wt% is attained, which corresponds to 3.5 V-atoms/nm^2 based on the support surface area. Above this level of loading, the amount of surface vanadia species is constant and then decreases.

DRIFT studies of ethane and propane adsorption on the 90Ti–W support and xV90Ti–W catalysts reveal the presence of several oxygenated adsorbed species. The possible pathways for their formation are shown in Fig. 12. The acetaldehyde- and acetone-adsorbed species were formed below 573 K. The acetaldehyde- and acetone-adsorbed species appear to be formed from the alkoxide species (ethoxide and isopropoxide), which in turn are formed by the abstraction of the hydrogen atom from the corresponding alkanes. At temperatures higher than 573 K, the acetaldehyde and acetone species are converted to acetate, formate, and cyclic anhydride adsorbed species, which are the precursors of the formation of carbon oxides. It also appears that the formation of the cyclic anhydride-adsorbed species is from the exposed support surface, which is suppressed by the presence of the surface vanadia species. In addition, adsorbed olefins/aldehydes or ketones associated with the conjugated C=O and C=C double bond are also detected.

The xV90Ti–W catalysts were tested for the propane ODH reaction. Contact time studies reveal that the propane conversion and propene yield depend on the vanadia loading. At the same contact time the conversion increases until the 7.5 wt% level of vanadia loading is attained, is constant for the 10 wt% loading and decreases thereafter. Analysis of various kinetic parameters determined for propane ODH reaction reveals that the kinetic parameters also depend on the vanadia loading. The pre-exponential factor for propene formation increases with vanadia loading. The lumped parameter, k_1/k_2 associated with propene yield at the same conversion also increases with increase in vanadia loading. The best in this series of catalysts is 10V90Ti–W since it provides the highest propane conversion measured at the same contact time and highest propene yield at the same conversion.

References

[1] E.A. Mamedov, V.C. Corberan, Appl. Catal. A: Gen. 127 (1995) 1–40.
[2] G. Deo, I.E. Wachs, J. Haber, Crit. Rev. Surf. Chem. 4 (1994) 141–187.
[3] M. Sanati, A. Anderson, Ind. Eng. Chem. Res. 30 (1991) 320–326.
[4] G.C. Bond, S.F. Tahir, Appl. Catal. 71 (1991) 1–31.
[5] G. Ramis, G. Busca, P. Forzatti, Appl. Catal. B: Environ. 1 (1992) L9–L13.
[6] J.P. Chen, R.T. Yang, Appl. Catal. A: Gen. 80 (1992) 135–148.
[7] J.B. Miller, E.I. Ko, Catal. Today 35 (1997) 269–292.
[8] X. Gao, S.R. Bare, J.L.G. Fierro, M.A. Bañares, I.E. Wachs, Phys. Chem. B 102 (1998) 5653–5666.
[9] A. Bialas, B. Borzecka-Prokop, A. Weselucha-Birczynska, J. Camra, M. Najbar, Catal. Today 119 (2007) 194–198.
[10] B. Mitra, I.E. Wachs, G. Deo, J. Catal. 240 (2006) 151–159.
[11] I.E. Wachs, T. Kim, E.I. Ross, Catal. Today 116 (2006) 162–168.
[12] L.J. Alenmany, L. Lietti, N. Ferlazzo, P. Forzatti, G. Busca, E. Giamello, F. Bregani, J. Catal. 155 (1995) 117–130.
[13] C. Resini, T. Montanari, G. Busca, J.M. Jehng, I.E. Wachs, Catal. Today 99 (2005) 105–114.
[14] G. Busca, E. Finocchio, V. Lorenzelli, G. Ramis, M. Baldi, Catal. Today 49 (1999) 453–465.
[15] P. Concepcion, P. Botella, J.M. Lopez Nieto, Appl. Catal. A: Gen. 278 (2004) 45–56.
[16] C. Li, Q. Xin, X. Guo, Catal. Lett. 12 (1992) 297–306.
[17] E. Finocchio, G. Busca, V. Lorenzelli, R.J. Willey, J. Catal. 151 (1995) 204–215.

[18] E. Heracleous, A.A. Lemonidou, J.A. Lercher, Appl. Catal. A: Gen. 264 (2004) 73–80.
[19] G. Busca, G. Ramis, V. Lorenzelli, J. Mol. Catal. 55 (1989) 1–11.
[20] D. Shee, T.V.M. Rao, G. Deo, Catal. Today 118 (2006) 288–297.
[21] K. Routray, G. Deo, J. AIChE 51 (2005) 1733–1746.
[22] R.P. Singh, M.A. Bañares, G. Deo, J. Catal. 233 (2005) 388–398.
[23] E.I. Ross-Medgaarden, I.E. Wachs, J. Phys. Chem. C 111 (2007) 15089–15099.
[24] M.A. Vuurman, D.J. Stufkens, A. Oskam, G. Deo, I.E. Wachs, J. Chem. Soc., Faraday Trans. 92 (1996) 3259–3265.
[25] N. Magg, B. Immaraporn, J.B. Giorgi, T. Schroeder, M. Baumer, J. Dobler, Z. Wu, E. Kondratenko, M. Cherian, M. Baerns, P.C. Stair, J. Sauer, H.J. Freund, J. Catal. 226 (2004) 88–100.
[26] D.C. Vermaire, P.C. van Berge, J. Catal. 116 (1989) 309–317.
[27] J. Engweiler, J. Harf, A. Baiker, J. Catal. 159 (1996) 259–269.
[28] D. Shee, G. Deo, Catal. Lett. 124 (2008) 340–351.
[29] M.A. Reiche, T. Bürgi, A. Baiker, A. Scholz, B. Schnyder, A. Wokaun, Appl. Catal. A: Gen. 198 (2000) 155–169.
[30] J. Raskó, J. Kiss, Appl. Catal. A: Gen. 287 (2005) 252–260.
[31] M.A. Hasan, M.I. Zaki, L. Pasupulety, J. Phys. Chem. B 106 (2002) 12747–12756.
[32] G. Busca, Catal. Today 27 (1996) 457–496.
[33] C. Xu, B.E. Koel, J. Chem. Phys. 102 (1995) 8158–8166.
[34] H.S. Fogler, Elements of Chemical Reaction Engineering, 3rd ed., Prentice-Hall of India Pvt. Ltd., New Delhi, 2002.